Surface Modification of UHSPE Fibers Through Allylamine Plasma Deposition. I. Infrared and ESCA Study of Allylamine Plasma Formed Polymers

Z.-F. LI and A. N. NETRAVALI*

Fiber Science Program, Department of Textiles and Apparel, Cornell University, Ithaca, New York 14853

SYNOPSIS

Allylamine ($CH_2{=}CH{-}CH_2{-}NH_2$) was polymerized through *rf* generated plasma at varying powers and times. Chemical groups and elemental compositions in the polymers were studied using ESCA and infrared spectroscopy. It was observed that plasma derived polymers contained a significant number of primary amines, along with some secondary and tertiary amines, imines, and nitrile groups. Plasma derived polymers had a complex structure and contained unsaturated groups. A considerable amount of oxygen, primarily from residual air in the plasma reaction chamber, and possibly from atmosphere when plasma polymers were exposed to air, was responsible for carbonyl, amide, ether, and hydroxyl groups found in the polymer structure. Some silicon was also detected in the plasma deposited films.

INTRODUCTION

Plasma is a cluster of particles including equal numbers of positive ions and electrons, free radicals, and natural species created by exciting a gas in electromagnetic or electrical fields. A variety of organic gases or vapors have been polymerized through their plasma state. Several authors have studied and reviewed the mechanisms of plasma polymerization.[1-3] Because of the complex nature of the plasma, mechanisms of plasma polymerization have not been completely understood. However, it is generally accepted that free radical and ionic initiation and propagation coexist in plasma polymerization and that polymerization takes place in gas phase as well as on the substrate surface.[4] Which of the two mechanisms dominates the polymerization depends on the conditions of the plasma discharge system, operational variables, and the chemical nature of the monomers.

Initially, when a gas is turned into a plasma, the probability of excited gas molecules to produce free radicals is higher than producing ions, because the energy required for bond dissociation to produce free radicals (3–4 eV) is much lower than that for ionization to produce ions and electrons (9–13 eV). Free radical density, at a pressure of 1 torr, was found by Kobayashi et al.[5] to be about 10^3–10^5 times that of ions. With the contribution of ionic species to polymerization being negligible, free radical polymerization was favored by Bell and coworkers.[5,6] High concentrations of free radicals, both in gaseous plasma and trapped in polymers, were detected by Yasuda and Hsu[7] using Electron Spin Resonance (ESR).

After plasma is created, various reactions, which are illustrated below, can occur through collisions and energy transfer among these species:

$$M + e^- = M\cdot + H^+ + 2e^-$$

$$M\cdot + H^+ = M^+ + H_2$$

$$M = M^+ + e^-$$

$$2M + e^- = M^+ + M^- + e^-$$

$$M + e^- = M^-$$

$$M\cdot + e^- = M^-$$

The neutral species (M) and free radicals ($M\cdot$) can be ionized (M^-, M^+) when they collide with high energy electrons. As a result, the ion population in-

* To whom correspondence should be addressed.

Journal of Applied Polymer Science, Vol. 44, 319-331 (1992)
 CCC 0021-8995/92/020319-13$04.00

creases and may exceed that of free radicals if the electron density and energy are high enough. Kinetically, ionic radial polymerization may predominate, even though free radical population is greater, if they have a lower rate of polymerization. Tickner[8] observed plasma glow deflected towards the negative electrode and most of the film deposited on the negative electrode in a 350 V dc electric field, due to the presence of positive ions. The predominant role of ionic species in polymerization is also supported by Smolinsky and Vasile,[9] based on mass spectrometric ion sampling analysis.

Plasma polymerization may yield film or powder depending upon experimental parameters such as flow rate and pressure. A pinhole-free solid film can often be obtained at a higher flow rate of the monomer and lower pressure, whereas powder is formed at a lower monomer flow rate and lower pressure.[10]

A review of the structure and morphology of plasma derived polymers have been presented by Shen and and Bell.[2] Plasma derived polymers are extremely irregular, highly cross-linked, and totally amorphous in nature. Also, functional groups that are not present in monomers often exist in polymer structures. Among various techniques to characterize polymers, Infrared (IR), Electron Spectroscopy for Chemical Analysis (ESCA), Nuclear Magnetic Resonance (NMR), and Mass Spectrometry (MS) have been particularly useful for obtaining empirical molecular structure.

Allylamine plasma was found to be polymerizable[11] and useful in preparation of reverse osmosis membranes.[12-14] Recently it has also been used to modify the surface of high strength fibers, such as glass fibers,[15] aramid fibers[16] and ultra-high-strength polyethylene fibers,[17] to increase their adhesion to resins in making fiber reinforced composites. The chemical structure of allylamine plasma polymer obtained at a single polymerization condition was characterized using IR and ESCA by Yasuda and coworkers[18] and by Peric et al.[12] This article extends the ESCA analysis further, to better understand the mechanism of allylamine plasma polymerization. The first part of the study characterizes the chemical structures of polymers formed at various conditions. The mechanisms of polymerization reactions are proposed.

EXPERIMENTAL

Material and Specimen Preparation

Allylamine ($H_2C{=}CH{-}CH_2{-}NH_2$) of 98% purity was obtained from Aldrich Chemical Corporation and was distilled before being used for plasma polymerization. Seventy-six mm diameter silicon wafers were cut into small pieces, 10 mm × 5 mm each, and were used as substrate for plasma polymerization and subsequently used for ESCA analysis. The silicon pieces were washed in acetone before using. They were glued to common optical microscopy glass slides using high vacuum grease. Wafer thin pieces of thicknesses less than 1 mm were cleaved from sodium chloride (NaCl) crystal and then kept in desiccators and used later for infrared analysis.

Plasma Polymerization

Plasma polymerization of allylamine was carried out using a Plasma Discharge System (PDS), Model 504, manufactured by LFE Corporation. The schematic of the system is shown in Figure 1. Four tubular quartz chambers were inductively coupled by 13.56 MHz *rf* generator. The inside chamber wall was covered with Kapton NH100 (polyimide) film, obtained from Du Pont de Nemours & Co., to prevent polymer from depositing on the chamber wall. The silicon wafers and sodium chloride crystals were placed in separate chambers. Since plasma polymerization is influenced by the geometrical position in the chambers, the silicon wafer and sodium crystals were put in the same place each time to avoid variation. Prior to introducing the allylamine vapor into the chambers, the system was vacuumed to 50 millitorrs. Allylamine vapor was then introduced and the pressure was maintained at 0.5 torr in the chamber by adjusting the flow meter control. The power was turned on when a steady pressure was established.

Polymer Film Characterization

Infrared spectra of plasma polymerized film, deposited on a sodium chloride crystal, were obtained using a dispersive Infrared Spectrophotometer Model 683 manufactured by Perkin Elmer Corporation, having a resolution of 4 wavenumbers. Several spectra were accumulated for each specimen.

Chemical compositions of plasma polymerized film deposited on silicon wafers were analyzed by ESCA using monochromatic Al K_α X-rays. The silicon wafers were cleaned by washing in acetone before using. The pressure in the main chamber was lowered to below 10^{-9} torr, after which the 10 KV X-ray source was turned on. ESCA spectra were recorded and analyzed, with a resolution of 2 eV, using an ESCA spectrometer Model SSX 100 manufactured by Surface Science Instruments Inc. Two tests

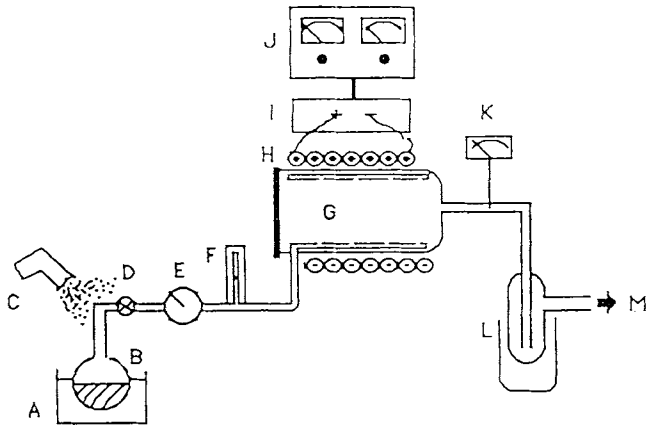

Figure 1 Schematic of the plasma discharge system, (A) Constant temperature bath, (B) Liquid monomer container, (C) Hot air blower, (D) Three-way stopcock, (E) Vacuum and pressure gauge, (F) Flow meter, (G) Glow discharge chamber, (H) Induction coils, (I) Matching box, (J) *Rf* generator, (K) Thermocouple vacuum gauge, (L) Liquid nitrogen container and gas trap, (M) To vacuum pump.

on each specimen at different places with a constant, 300 μm, spot diameter were run and the averages of relative compositions were used.

Polymer film thicknesses on silicon wafers were measured by an Inteferometer Model Leitz MPV-SP that scans from 400 to 800 nm wavelengths (white light). Refractive index of plasma deposited films was assumed to be 1.54, which is common for most polymers. Three to four measurements were taken for each sample at different places.

RESULTS AND DISCUSSIONS

General Observations of Plasma Polymerization

After turning the *rf* generator on at sufficiently high power input of approximately 20–25 W, at a pressure of 0.5 torr, the glow discharge appeared. The light blue color of the glow at 30 W changed to light purple at 45 W and ultimately turned to bright pink at 70 W. The glow intensity increased as the power increased and decreased as the pressure in the chamber decreased.

Polymeric film, as well as some powder depositions, were found on substrates under different conditions. The powder exclusively deposited on the bottom left end in the chamber from where the monomer vapor was fed, as illustrated in Figure 1. This is presumably due to lower vapor flow rate when gaseous phase polymerization is predominant, as discussed by Kobayashi et al.[10] Transparent and yellowish polymer films were deposited on the silicon wafers, NaCl crystals, and the fiber specimens that were placed in the middle of the chamber.

Once adjusted, the pressure in the chamber could be maintained at a constant value for 5 to 10 min. However, it dropped gradually from 0.5 torr to 0.2 torr at longer times, such as 20 and 40 min, if unattended. The flow rate was continuously monitored and readjusted to obtain a pressure of 0.5 torr. The decrease in pressure means that the rate of polymerization is higher than the feeding rate of monomer. Under the present conditions, the polymerization is believed to have been initiated both in gaseous phase and on the surface of substrates.

Rate of Plasma Polymer Deposition

The rate of plasma polymerization depends on parameters such as the flow rate of monomer, pressure, power input, time, and temperature. The plasma polymerization process being very complex, it is difficult to interpret the rate of polymerization in terms of initiation, propagation, and termination rates as in conventional radical polymerization. In this study, the bulk rate of polymerization is measured in terms of the rate of polymer film deposition. The effect of time on the rate of polymer film deposition at 45 W power input is shown in Figure 2. The effect of power input on the rate of polymer deposition is shown in Figure 3. It can be seen from Figure 2 that the film thickness increases linearly at a rate of 4.6 nm/min. The rate of deposition increases with the power input at a rate of 0.095 nm/min/watt, as shown in Figure 3. Such a linear effect of power indicates that

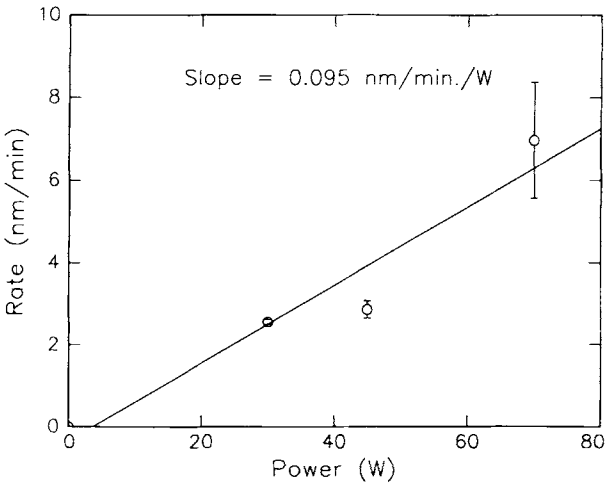

Figure 2 Effect of power input on rate of polymer deposition.

the plasma polymerization is still in the power deficient region as defined by Yasuda and Wang.[19]

IR Analysis

The infrared spectra of allylamine and the plasma derived polymers are compared in Figure 4. In Figures 5 and 6 we show the infrared spectra of plasma derived polymers under different conditions. It can be seen from Figures 5 and 6 that the polymers obtained under all reaction conditions have similar peak characteristics, indicating similar structural groups. The relative number of these groups, however, varies.

A summary of wavenumbers and the vibrational mode assignments are shown in Table I. The broad band observed at 3250 cm^{-1} wavenumber is a result of the stretching of N—H bonds from primary, secondary amines, and possibly O—H groups. Gombotz and Hoffman,[20] who plasma polymerized allylamine on various substrates, also reported a band between 3100 and 3600 cm^{-1} due to N—H stretch. Their results also showed that the polymer composition remained the same for any substrate. The peak at 1590 cm^{-1}, corresponding to the bending of N—H bonds in primary amines, is seen in allylamine as well as in all the polymers. Peak at 795 cm^{-1} is most likely from out-of-plane bending of N—H groups from primary and secondary amines.

Strong absorption corresponding to C=C stretching at 1640 cm^{-1} and H—H bending at 1590 cm^{-1} present in allylamine are also seen in the polymers. However, the broadness of these peaks in polymers suggests a complex structure and various conjugations in which these groups exist. Other peaks that appear in the polymer structure, but are not present in allylamine, are due to carbonyl (C=O, 1710 cm^{-1}), amide (—C—N, 1690 cm^{-1}), and imine (—C=N—, 1675 cm^{-1}). Conjugation among these groups shifts their respective peaks to lower wavenumbers.

The C—H bending in methylene (—CH_2—, 1460 cm^{-1}) and in vinyl groups (—$CH=CH_2$, 1430 cm^{-1}) are present in allylamine as well as in the polymer spectra (Fig. 4), whereas peak at 1375 cm^{-1} wavenumber, characteristic of methyl groups, is only found in polymers.

Another change in peaks from monomer to polymer is the disappearance of peaks at 990 cm^{-1} and 910 cm^{-1}, corresponding to out-of-plane C—H bending in vinyl groups in allylamine, which suggests a reduction in vinyl groups in the polymers probably due to di, tri, or tetra substitutions. The peak at 950 cm^{-1}, characteristic of out-of-plane C—H bending in trans-1,2 disubstituted >C=C< bonds, is seen in the polymers obtained at lower power and lower times, but disappears at higher power or longer times. This suggests that hydrogens in >C=CH_2 groups are substituted with other groups.

It can be seen from Figures 5 and 6 that peak at 2180 cm^{-1} wavenumber appears only in the polymers obtained at 70 W for 10 min, at 45 W for 20 min, and at 45 W for 40 min. This peak may be assigned to the nitrile group (C≡N) and alkyne (C≡C) groups and conjugated with carbonyl or ethylene groups conjugated with carbonyl or ethylene groups. This suggests that more hydrogens are abstracted from monomers and growing chains at higher power inputs and at longer times, resulting in higher number of double and triple bonds.

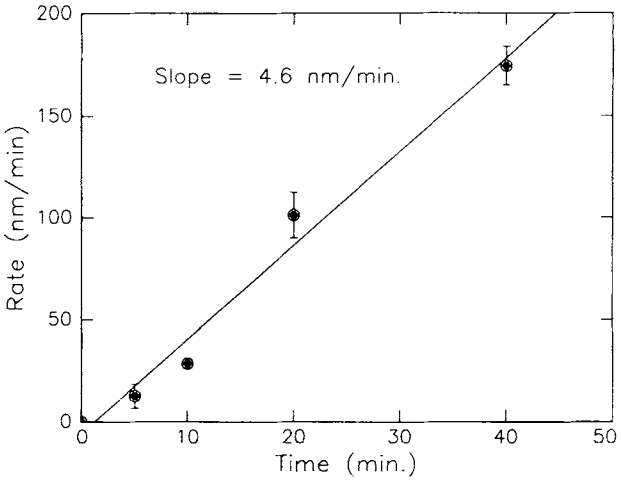

Figure 3 Effect of exposure time on rate of polymer deposition.

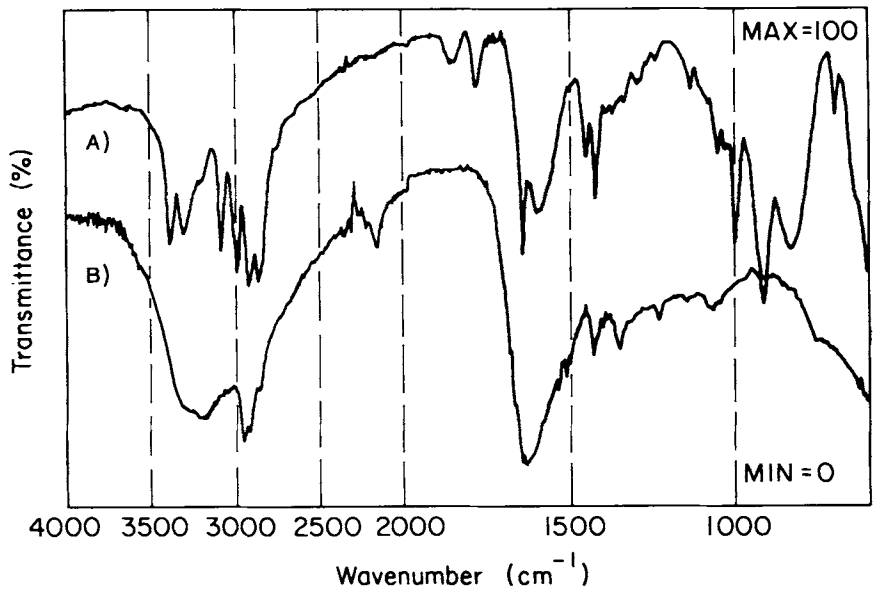

Figure 4 Infrared spectra of (A) Allylamine liquid, and (B) its plasma polymer formed at 45 W for 40 min.

ESCA Analysis of Allylamine Plasma Formed Polymers

The scanning of the energy spectrum of photoelectrons originating from the specimen over 0 to 1000 eV binding energy produces 5 distinct peaks corresponding to C_{1s}, N_{1s}, O_{1s}, Si_{2s}, and Si_{2p}. The peaks of Si_{2s} and Si_{2p} are not expected in the polymer films because ESCA can only measure the surface chemical compositions up to a depth of less than 100 Å, whereas the thinnest polymer film obtained in the present study is 126 Å thick.[17] Yeh and Yasuda,[21] who used silicone rubber substrates with a glass transition temperature lower than the experimental

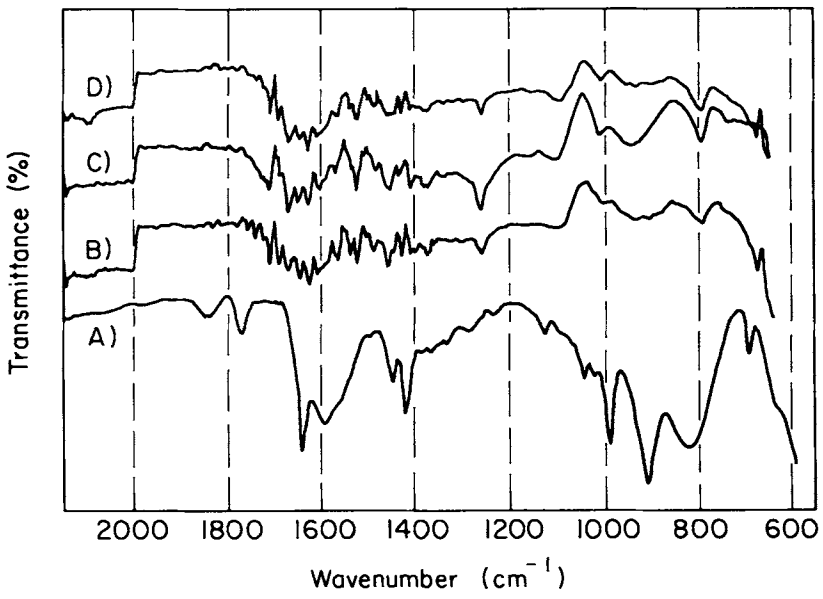

Figure 5 Infrared spectra from 2300 cm^{-1} to 600 cm^{-1} wavenumbers of allylamine liquid (A) and plasma polymers formed at different power inputs: (B) 30 W, (C) 45 W, (D) 70 W, for 10 min.

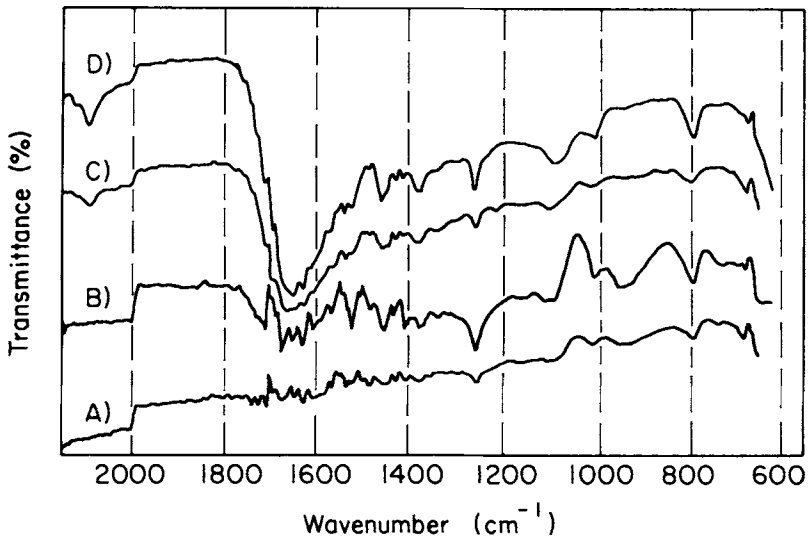

Figure 6 Infrared spectra from 2300 cm^{-1} to 600 cm^{-1} wavenumbers of allylamine plasma polymers for exposure times of (A) 5 min, (B) 10 min, (C) 20 min, (D) 40 min formed at 45 W.

temperature, found a considerable amount of silicon in the deposited fluorocarbon films due to interfacial diffusion. In the present case, interfacial diffusion of silicon from the wafer may not be possible. The % silicon component, however, is below 10% and probably is a result of the sputtering by the energetic species within the allylamine plasma or may have come from the dust sitting on the specimen.

It may also be noted that the Si_{2p} peak was obtained at a binding energy value of 102.2 eV, indicating oxidized silicon. Binding energy for pure silicon is 99.2 eV. The ratio of silicon to oxygen in the specimen is approximately equal to $\Delta E_b/2.2$, where ΔE_b is the chemical shift due to oxidation.[22] In all the polymer film spectra, only the peaks for oxidized Si (102.2 eV for Si_{2p} and 153.3 eV for Si_{2s}) are seen.

Table II gives the elemental composition of N, C, O, and Si and their ratios in polymer films for all conditions. The ratio of nitrogen/carbon, about 0.20, is approximately the same for polymer films formed under all conditions of power and time. However, this ratio is much smaller than 0.33 for allylamine monomer. This suggests that chain scissions occur at C—N bonds during polymerization, resulting in a loss of about one third of nitrogen. This can be explained easily since the dissociation of the C—N bond is energetically more favorable than the C—C bond. It may be noted that with the increase in the power the nitrogen content decreases from 12.7% for 30 Watts to 10.5% for 70 Watts, indicating a higher loss at a higher power.

The incorporation of oxygen is primarily a result of the residual air in the reaction chamber and to a small extent by the oxidation of the polymer films when exposed to air. At the beginning of the reaction, oxygen in the reaction chamber is incorporated in the polymer deposition. With time, as the polymer layer builds up, oxygen in the chamber is no longer available to be incorporated into the top layer of polymer deposition. When the specimen is taken out of the chamber, the free radicals still present in the film can be oxidized. Thus, oxygen in the top layer comes from oxidation of the polymer when exposed to air while oxygen in the bottom layer is mainly a result of residual air in the plasma chamber.

The deconvoluted views of individual peaks are shown in Figures 7–11. To eliminate the effect of static charge, which increases the binding energy values, all peaks of Si_{2p} in all polymers are shifted to 102.2 eV, which is the peak binding energy of oxidized silicon in the control substrate. Other peaks have also been shifted correspondingly. The silicon wafer being a semiconductor, static charges are negligible. However, the polymer films are non-conducting and can accumulate static charge. The peak binding energies and the full width at half maximum (FWHM) are shown in Table III. The peak binding energies of C_{1s}, N_{1s}, and O_{1s} after shifting match typical values found in the references and handbooks.[23-27]

The FWHMs of C_{1s} of polymers are over twice as large as that of control. Broadness of the peaks

Table I Peak Assignments in Infrared Spectra

Wavenumber (cm 1)	Structure	Vibrational Mode
3250	N—H & O—H	Stretching
3040	C—H in =C—H	Stretching
2960, 2930, 2880	C—H in CH_2 & CH_3	Stretching
2180	C≡N (Conjugated)	Stretching
1710	C=O	Stretching
1690	C=O (Conjugated)	Stretching
	O=C—N	
1675	C=N	Stretching
1640	C=C	Stretching
	O=C—N (Conjugated)	Stretching
1630	C=C (Conjugated)	Stretching
1590	N—H in C=N—H	Bending
	C=C (conjugated)	Stretching
1565	N—H in $—NH_2$	Bending
1460	C—H in CH_2	Scissoring Bending
	in CH_3	Asymmetrical Bending
1375	C—H in CH_3	Symmetrical Bending
990, 950, 910	C—H in trans 1, 2 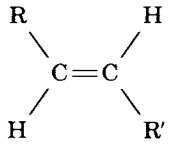	
795	N—O	Out-of-plane Bending
	N—H	Stretching
		Out-of-plane Bending
990, 950, 910	C—H in 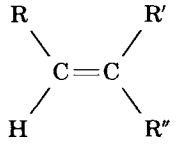	Out-of-plane Bending

indicate that polymers have a very complex structure. It may be recalled that a similar effect was also seen in infrared analysis. The C_{1s} peak at 285 eV, as shown in Figure 8, can be resolved into a major peak for alkyls and alkenes (C=C) at 285.0 eV, and other peaks such as amines (—C—N—) at 286.2

Table II Elemental Composition of Plasma Polymerized Films Obtained from ESCA

Experimental Condition		Elemental Composition				Composition Ratio		
Power (W)	Time (min)	C (%)	N (%)	O (%)	Si (%)	N/C	O/C	Si/C
30	10	66.82	12.70	14.07	6.41	0.19	0.21	0.10
45	10	58.48	11.59	21.12	8.82	0.20	0.36	0.16
70	10	63.22	10.50	16.70	9.58	0.17	0.26	0.15
45	5	59.56	11.42	21.04	7.98	0.19	0.35	0.15
45	10	58.48	11.59	21.12	8.82	0.20	0.36	0.16
45	20	65.95	14.02	14.67	5.35	0.21	0.24	0.16
45	40	59.78	12.99	18.23	9.00	0.22	0.31	0.16

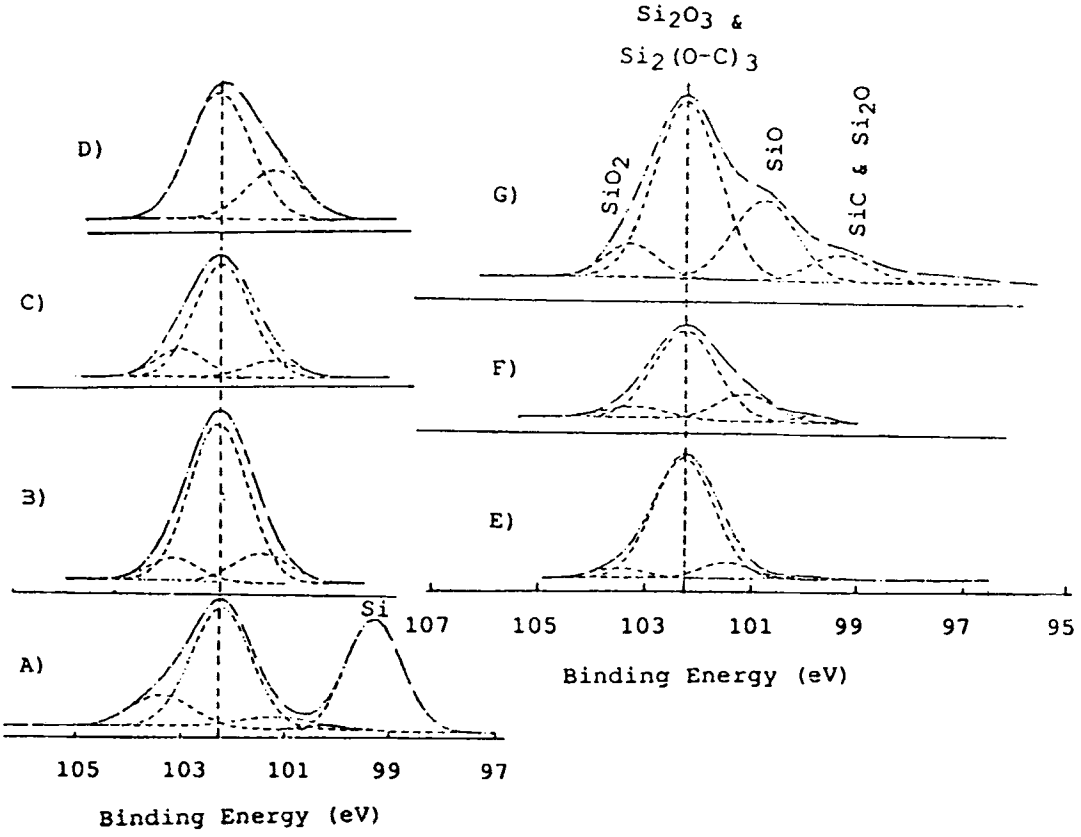

Figure 7 Si_{2p} spectra for allylamine plasma polymers, (A) Control, (B) 30 W, 10 min, (C) 45 W, 10 min, (D) 70 W, 10 min, (E) 45 W, 5 min, (F) 45 W, 20 min, (G) 45 W, 40 min.

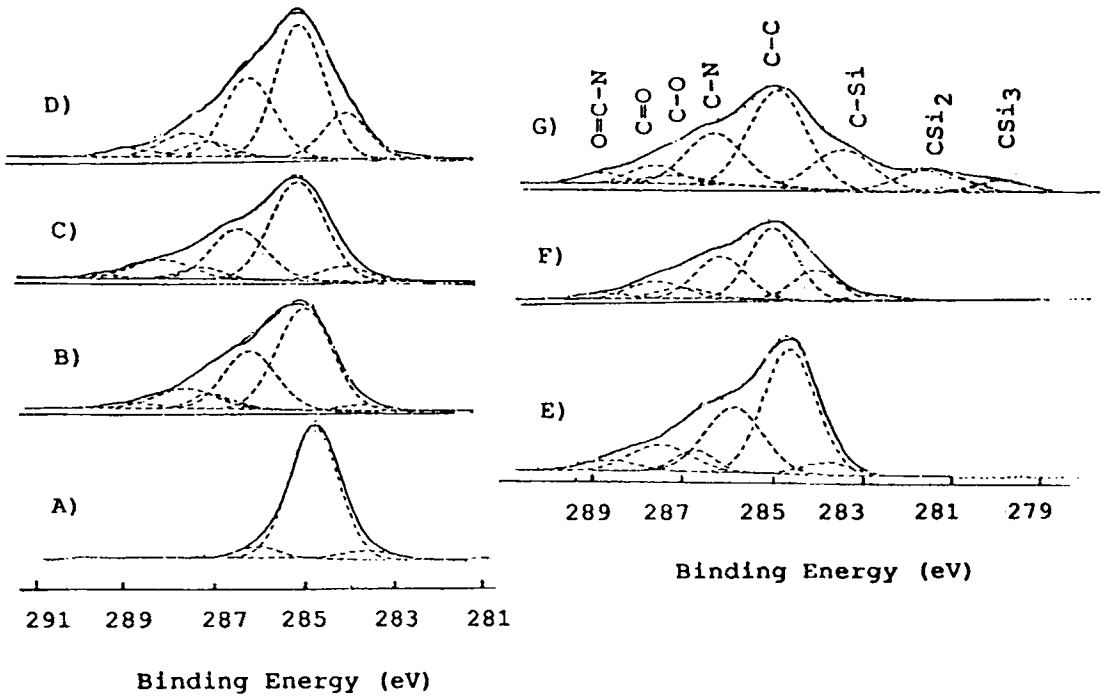

Figure 8 C_{1s} spectra for allylamine plasma polymers, (A) Control, (B) 30 W, 10 min, (C) 45 W, 10 min, (D) 70 W, 10 min, (E) 45 W, 5 min, (F) 45 W, 20 min, (G) 45 W, 40 min.

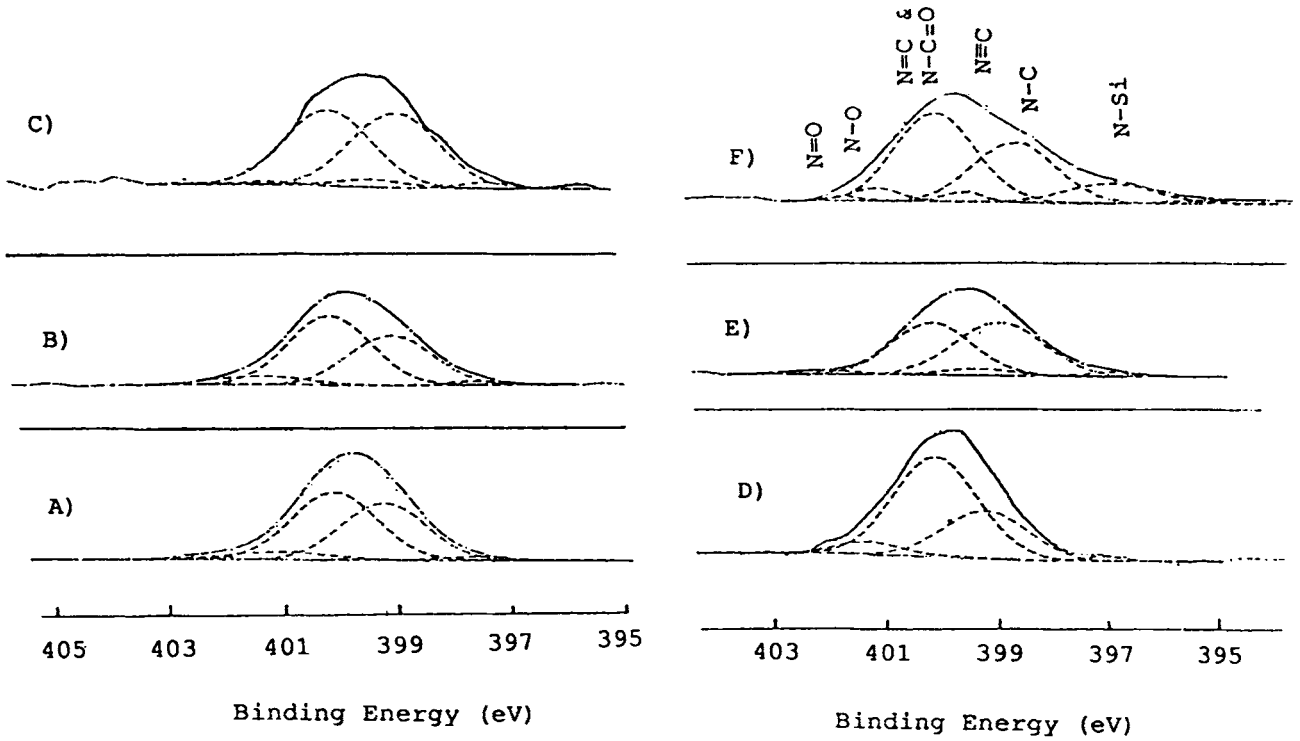

Figure 9 N_{1s} spectra for allylamine plasma polymers, (A) 30 W, 10 min, (B) 45 W, 10 min, (C) 70 W, 10 min, (D) 45 W, 5 min, (E) 45 W, 20 min, (F) 45 W, 40 min.

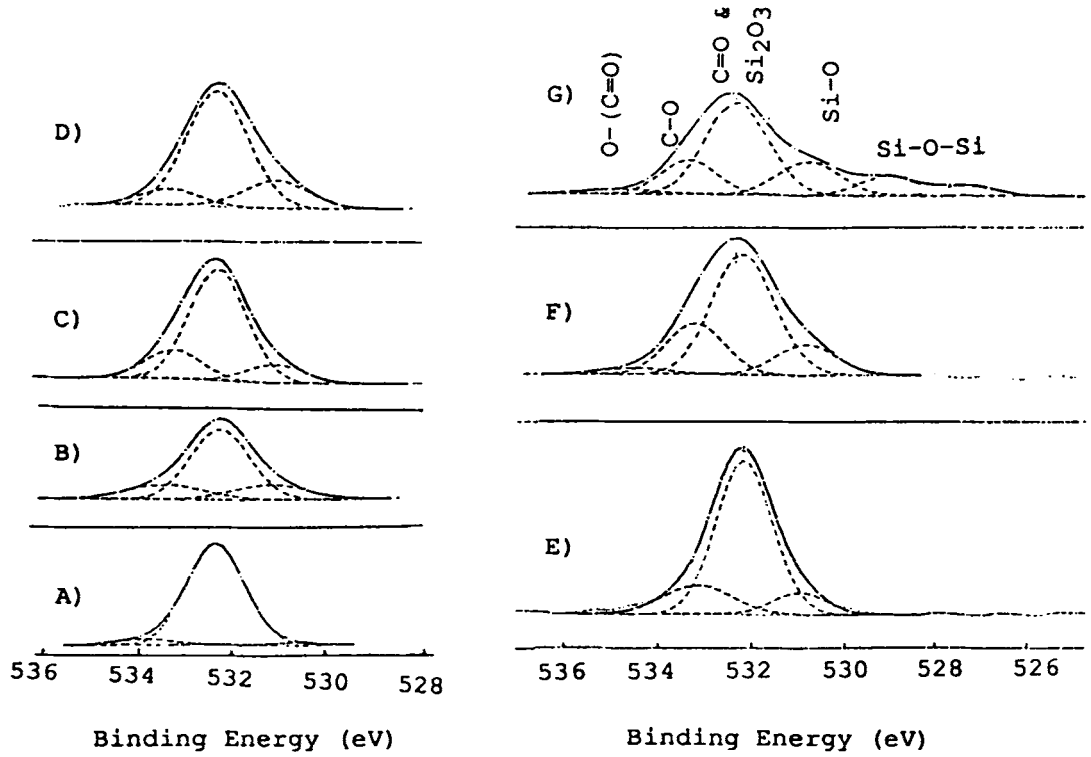

Figure 10 O_{1s} spectra for allylamine plasma polymers, (A) Control, (B) 30 W, 10 min, (C) 45 W, 10 min, (D) 70 W, 10 min, (E) 45 W, 5 min, (F) 45 W, 20 min, (G) 45 W, 40 min.

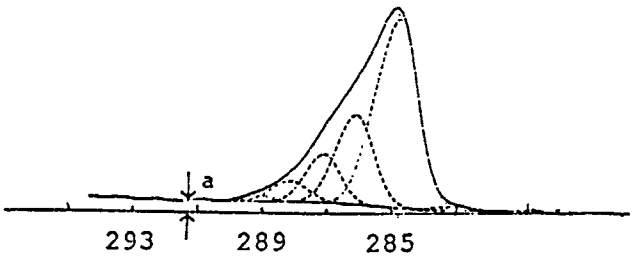

Figure 11 Asymmetrical tail structure arising from conjugation of unsaturated bonds in allylamine plasma polymer.

eV, carbonyl (C=O) at 287.8 eV, ether and alcohol (C—O) at 287 eV, amide (O=C–NH) at 289 eV, and silicon carbide (SiC_x) at 282 ± 1 eV in decreasing order of their relative peak areas.

N_{1s} peaks at peak binding energies of 399.7 eV can be deconvoluted into two major peaks at 399 eV for amine groups, at 400.1 eV for imine and amide groups, and into two small peaks corresponding to N—O and N—Si as shown in Figure 9. The FWHM for the individual peaks lies within 1.6–1.8 eV. The number of amide groups is 10–20% of the sum of C—N and C=N groups. It can, therefore, be concluded that nitrogen in the plasma polymers mostly exists in amine, imine, and amide forms. Other possible structures, such as N—C—O, C—N=N—C also result in N_{1s} peak at about 400 eV. Clark and Harrison[27] showed that the N_{1s} peak shifted slightly to the lower binding energy side only by about 0.2 eV primary amines to secondary amines and tertiary amines making it difficult to deconvolute the C—N peak into primary amine, secondary amine, and tertiary amine.

The O_{1s} peak at 532.2 eV can be deconvoluted into a major peak for carbonyl (C=O) at 532.2 eV and two peaks for C—O at 533.3 eV and O—Si at 531 eV, as shown in Figure 10. The O_{1s} peak of silicon oxide from silicon substrate also has a predominant peak at 532.2 eV, as shown in Figure 10(A). High relative peak area at 532.2 eV (50–70%) for polymer films is a result of both carbonyl and silicon oxide. The ester oxygen in carboxyl groups exhibits a small peak at 534.5 eV and exists only in polymers formed at longer times. It may be concluded from these observations that oxygen exists mostly in the form of carbonyl and ether groups.

It can be seen from Table III that FWHMs of all peaks increase with time and power. The increase in FWHM is due to the complex structure which results in peak shifts in either direction. For instance, in N_{1s}, as time and power increase, the total

Table III Peak Binding Energies and Full Width at Half Maximum (FWHM)

Power (W)/Time (m)		0/0	30/10	45/10	70/10	45/5	45/20	45/40
Si_{2p}	Peak (eV)	102.2[a]	102.2	102.2	102.2	102.2	102.2	102.2
	FWHM (eV)	1.56[a]	1.56	1.62	1.70	1.56	1.81	2.13
Si_{2s}	Peak (eV)	153.3[a]	153.3	153.3	153.1	153.4	153.3	153.2
	FWHM (eV)	2.12[a]	2.13	2.27	2.27	2.00	2.57	3.00
C_{1s}	Peak (eV)		284.9	285.0	285.0	284.7	284.6	285.0
	FWHM (eV)		2.50	2.50	2.50	2.50	2.83	3.23
N_{1s}	Peak (eV)		399.5	399.8	399.5	399.7	399.7	399.9
	FWHM (eV)		2.20	2.30	2.55	1.95	2.29	2.84
O_{1s}	Peak (eV)		532.2	532.2	532.2	532.2	532.2	532.1
	FWHM (eV)		1.99	1.99	1.99	1.77	2.34	2.34

[a] Data taken from oxidized silicon peak.

concentration of N—O, N—Si groups, secondary amines, and tertiary amines, and consequently the intensities of these peaks, increase. When combined with the main amine peak, the N_{1s} peak widens. FWHMs of O_{1s} and C_{1s} remain the same at the different power input. This is because the peaks arising from carbonyl and alkyls and alkene are so dominant that other peaks have no significant effect on peak width.

From the infrared spectra, it was concluded that the conjugation among C=C, C=O, and C=N possibly exists in polymer chains. The electron shake-up transition arising from the conjugations produces a small satellite peak.[28] Munro and Grunwald[29] argued that if the conjugation length increases along the polymer chain, the satellite peak cannot be observed. Instead a long tail appears at the higher binding energy side. In C_{1s}, if there is no shake-up transition as in polyethylene, the tail arising from the inelastic collision of electrons appears from ~293 eV.[29] The allylamine plasma polymers exhibit asymmetrical C_{1s} peaks with small tails from 289 eV, confirming the conjugation of unsaturated bonds in polymer structures. The acrylonitrile plasma polymer was also shown to have an asymmetrical tail by Munro and Grunwald.[29] The asymmetrical tail structures are distinct in conjugated aromatic polymers.[30,31] N_{1s} and O_{1s} all have such asymmetric tails if N and O are a part of conjugation.[30,31] The N_{1s} peaks do not show the "tail." Instead, there are a few small peaks, suggesting that the length of conjugation arising from C=N is small and the amount of C=N is small compared to that of the C=C bonds.

Mechanism of Plasma Polymerization

From IR and ESCA analyses, the formation of plasma polymer structures may be proposed by the following reaction schemes:

$$CH_2{=}CH{-}CH_2{-} \rightarrow \dot{C}H_2{-}\dot{C}H{-}CH_2{-}$$

$$\dot{C}H_2{-}\dot{C}H{-}CH_2{-} \xrightarrow{\text{Propagation}} \dot{C}H_2{-}\dot{C}H{-}\dot{C}H_2{-}$$

$$\dot{C}H_2{-}\dot{C}H{-}CH_2{-} \xrightarrow{\text{H Abstraction}} \dot{C}H_2{-}\dot{C}H{-}\dot{C}H{-}$$

$$\dot{C}H_2{-}\dot{C}H{-}CH_2{-} \xrightarrow{\text{Chain Scission}} \dot{C}H_2{-}\dot{C}H + \cdot CH_2{-} \quad (1)$$

$$-CH_2{-}NH_2 \xrightarrow{} -\dot{C}H{-}\dot{N}H \rightarrow$$

$$-CH_2{-}NH_2 \xrightarrow{} -\dot{C}H{-}\dot{N}H \rightarrow$$

$$-CH_2{-}NH_2 \xrightarrow{\text{Chain Scission}} -\dot{C}H + \cdot NH_2 \rightarrow$$

→ Further H abstraction and chain scission and propagation (2)

The above reactions result in chain growth and crosslinks, with a large number of free radicals being trapped in the chains. When the plasma discharge is turned off, free radicals de-excite and can combine to form double and triple bonds and crosslinks as follows:

$$-\dot{C}-\dot{C}- \rightarrow \quad \diagdown C{=}C \diagup$$

$$-C\cdot + \cdot C- \rightarrow -C-C-$$

$$-\dot{C}-\dot{N} \rightarrow \quad \diagdown C{=}N-$$

$$-\dot{C}-\dot{N} \rightarrow -C{\equiv}N \quad (3)$$

Bell et al.[11] proposed a reverse reaction route in which the allylamine monomers are first converted to imines and nitriles, C=C bonds are converted to C≡C and then are polymerized, resulting in a large number of unsaturated groups. This would mean that polymers formed even at very short times would contain considerable amounts of unsaturated groups including C=N, C≡C, and C≡N in polymers. However, this study shows that only a small number of nitrile groups are found in polymers formed at longer times and at higher power inputs.

Free radicals in polymer chains can also react with hydrogen radicals in gaseous phase, creating methyl and primary amines:

$$-CH_2-\dot{C}H_2 + H\cdot \rightarrow -CH_2-CH_3$$

$$-\dot{N}-H + H\cdot \rightarrow -N\begin{matrix}H\\H\end{matrix} \quad (4)$$

Another way primary amine groups could be incorporated in polymers is by radicals in polymer chains reacting with monomers when plasma discharge is turned off as follows:

$$-CH_2-\dot{C}H- + CH_2{=}CH-CH_2-NH_2 \rightarrow$$

$$\rightarrow -CH_2-CH-$$

$$\qquad\qquad\quad |$$

$$\qquad\qquad CH_2-\dot{C}H-CH_2-NH_2 \quad (5)$$

The above reactions cease when substrates are taken out and exposed to air. However, there still remain

a large number of free radicals trapped in polymers chains. Neighboring free radicals can recombine, but those separated by at least two bonds cannot recombine to form unsaturated bonds or crosslinks. These remaining free radicals can be oxidized into hydroxyl, carbonyl, etc. when exposed to air.

At the beginning of the plasma discharge, the nitrogen and oxygen in residual air can combine with radicals to form peroxide, carbonyl, ether, etc. as follows:

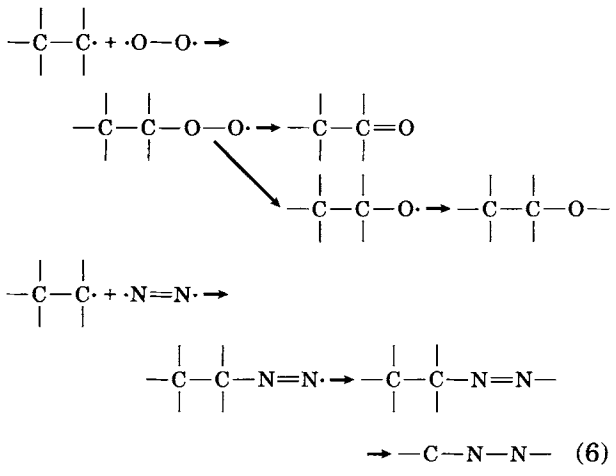

(6)

CONCLUSIONS

Allylamine plasma polymer films contain considerable amounts of primary amine and imine groups along with some amides, secondary, and tertiary amine groups. A small number of nitrile groups were found in polymers formed at high power and long times.

Groups containing oxygen, such as carbonyl, ether, and hydroxyl groups, were also present in the polymer. Oxygen from the residual air in the polymerization chamber and oxidation of plasma derived polymers when exposed to the atmosphere were responsible for the oxygen containing groups.

The elemental composition of plasma polymers obtained under different conditions showed the N/C ratio to be approximately the same for all the polymers. The O/N and O/C ratios tend to decrease with polymerization time.

Various unsaturated groups, such as C=C, C=N, C=O and conjugation, created complex polymer structures and resulted in a peak with an asymmetrical tail for C_{1s}.

Some amount of silicon, possibly from dust in the air or a result of the sputtering by energetic species within the allylamine plasma, was detected in the form of silicon carbides and silicon nitrides.

This work was primarily funded by the Small Grants Committee of the College of Human Ecology. Authors would like to thank Dr. Bishun Khare of the Laboratory of Planetary Research for providing plasma polymerization equipment and Mr. Kelly Brower for technical assistance. We would also like to thank Professor R. Buhrman of Applied Engineering Physics for providing ESCA equipment in his laboratory and Tony Huang and Hans Hallen for technical assistance. We would like to thank Yarrow Namaste for measuring the film thicknesses.

REFERENCES

1. M. Millard, In *Techniques and Applications of Plasma Chemistry*, J. R. Hollahan and A. T. Bell, Eds., Wiley, New York, 1974.
2. M. Shen and A. T. Bell, In *Plasma Polymerization*, ACS Symposium Series No. 108, ACS, Washington, DC 1979.
3. A. M. Mearns, *Thin Solid Film*, **3**, 201 (1969).
4. H. Yasuda, *Plasma Polymerization*, Academic, Orlando, FL, 1985.
5. H. Kobayashi, A. T. Bell, and M. Shen, *Macromolecules*, **7**, 277 (1974).
6. J. M. Tibbitt, R. Jensen, A. T. Bell, and M. Shen, *Macromolecules*, **10**, 647 (1977).
7. H. Yasuda and T. Hsu, *J. Polym. Sci. Polym. Chem. Ed.*, **15**, 81 (1977).
8. A. W. Tickner, *Can. J. Chem.*, **39**, 87 (1961).
9. G. Smolinsky and M. J. Vasile, *Intl. J. Mass Spectrom. Ion Phys.*, **12**, 147 (1973).
10. H. Kobayashi, A. T. Bell, and M. Shen, *J. Appl. Polym. Sci.*, **17**, 885 (1973).
11. H. Yasuda and C. E. Lamaze, *J. Appl. Polym. Sci.*, **17**, 1519 (1973).
12. D. Peric, A. T. Bell, and M. Shen, *J. Appl. Polym. Sci.*, **21**, 2661 (1977).
13. A. T. Bell, Y. Wydeven, and C. C. Johnson, *J. Appl. Polym. Sci.*, **19**, 1911 (1975).
14. J. R. Hollahan and T. Wydeven, *Science*, **179**, 500 (1973).
15. V. Krishnamurthy and I. L. Kamel, *33rd Intl. SAMPE Symposium*, Anaheim, CA, 1988, p. 560.
16. M. R. Wertheimer and H. P. Schreiber, *J. Appl. Polym. Sci.*, **26**, 2087 (1981).
17. Z.-F. Li and A. N. Netravali, *J. Appl. Polym. Sci.*, in press (1989).
18. H. Yasuda, M. D. Bumgarner, H. C. Marsh, and N. Morosoff, *J. Polym. Sci. Polym. Chem. Ed.*, **14**, 195 (1976).
19. H. Yasuda and C. R. Wang, *J. Polym. Sci. Polym. Chem. Ed.*, **23**, 87 (1985).
20. W. R. Gombotz and A. S. Hoffman, In *J. Appl. Polym.*

Sci. Appl. Polym. Symp., No. 42, H. K. Yasuda, Ed., Wiley, New York, 1988, p. 285.
21. Y.-S. Yeh and H. Yasuda, *J. Polym. Sci. Part A Polym. Chem.*, **24,** 3233 (1986).
22. J. H. Thomas III, In *Applied Electron Spectroscopy for Chemical Analysis,* H. Windawi and F. F.-L. Ho, Eds., Wiley, New York, 1982.
23. K. Siegbahn, C. Nordling, A. Fahlman, R. Nordberg, K. Hamrin, J. Heelman, G. Johansson, T. Bergmark, S. Karlsson, I. Lindgren, and B. Lindberg, *ESCA: Atomic, Molecular, and Solid State Structure Studied by Means of Electron Spectrosocpy,* Almqvist and Wiksells, Uppsala, Sweden, 1967.
24. D. Briggs and M. P. Seah, *Practical Surface Analysis by Auger and X-ray Photoelectron Spectroscopy,* Wiley, New York, 1983.
25. H. Windawi and F. F.-L. Ho, Eds., *Applied Electron Spectroscopy for Chemical Analysis,* Wiley, New York, 1982.
26. D. T. Clark and A. Dilks, *J. Polym. Sci. Polym. Chem. Ed.,* **17,** 957 (1979).
27. D. T. Clark and A. Harrison, *J. Polym. Sci. Polym. Chem. Ed.,* **19,** 1945 (1981).
28. D. T. Clark, *Adv. Polym. Sci.,* **24,** 125 (1977).
29. H. S. Munro and H. Grunwald, *J. Polym. Sci. Polym. Chem. Ed.* **23,** 479 (1985).
30. T. Takahagi, I. Shimada, M. Fukuhara, K. Morita, and A. Ishitani, *J. Polym. Sci. Polym. Chem.*, **24,** 3101 (1986).
31. A. Dilks and D. T. Clark, *J. Polym. Sci. Polym. Chem. Eds.*, **19,** 2847 (1981).

Received June 6, 1989
Accepted February 21, 1991